Antibacterial photosensitization through activation of coproporphyrinogen oxidase

Matthew C. Surdel[a], Dennis J. Horvath Jr.[a], Lisa J. Lojek[a], Audra R. Fullen[a], Jocelyn Simpson[a], Brendan F. Dutter[b,c], Kenneth J. Salleng[a], Jeremy B. Ford[d], J. Logan Jenkins[d], Raju Nagarajan[e], Pedro L. Teixeira[f], Matthew Albertolle[c,g], Ivelin S. Georgiev[a,e,h], E. Duco Jansen[d], Gary A. Sulikowski[b,c], D. Borden Lacy[a,d], Harry A. Dailey[i,j,k], and Eric P. Skaar[a,1]

[a]Department of Pathology, Microbiology, and Immunology, Vanderbilt University Medical Center, Nashville, TN 37232; [b]Department of Chemistry, Vanderbilt University, Nashville, TN 37232; [c]Vanderbilt Institute for Chemical Biology, Nashville, TN 37232; [d]Department of Biomedical Engineering, Vanderbilt University, Nashville, TN 37232; [e]Vanderbilt Vaccine Center, Vanderbilt University Medical Center, Nashville, TN 37232; [f]Biomedical Informatics, Vanderbilt University School of Medicine, Nashville, TN 37203; [g]Department of Biochemistry, Vanderbilt University, Nashville, TN 37232; [h]Department of Electrical Engineering and Computer Science, Vanderbilt University, Nashville, TN 37232; [i]Biomedical and Health Sciences Institute, University of Georgia, Athens, GA 30602; [j]Department of Microbiology, University of Georgia, Athens, GA 30602; and [k]Department of Biochemistry and Molecular Biology, University of Georgia, Athens, GA 30602

Edited by Ferric C. Fang, University of Washington School of Medicine, Seattle, WA, and accepted by Editorial Board Member Carl F. Nathan June 26, 2017 (received for review January 10, 2017)

Gram-positive bacteria cause the majority of skin and soft tissue infections (SSTIs), resulting in the most common reason for clinic visits in the United States. Recently, it was discovered that Gram-positive pathogens use a unique heme biosynthesis pathway, which implicates this pathway as a target for development of antibacterial therapies. We report here the identification of a small-molecule activator of coproporphyrinogen oxidase (CgoX) from Gram-positive bacteria, an enzyme essential for heme biosynthesis. Activation of CgoX induces accumulation of coproporphyrin III and leads to photosensitization of Gram-positive pathogens. In combination with light, CgoX activation reduces bacterial burden in murine models of SSTI. Thus, small-molecule activation of CgoX represents an effective strategy for the development of light-based antimicrobial therapies.

bacteria | photosensitization | CgoX | heme | antibiotic

Skin and soft tissue infections (SSTIs) are responsible for a majority of visits to hospitals and clinics in the United States, accounting for ∼14 million ambulatory care visits each year (1). Furthermore, ∼10% of hospitalized patients suffer from an SSTI (1). These infections are typically caused by Gram-positive bacteria including *Staphylococcus aureus*, *Staphylococcus epidermidis*, *Propionibacterium acnes*, and *Bacillus anthracis*, the causative agents of "staph infections," hospital-acquired infections, acne, and cutaneous anthrax, respectively (1–4). *S. aureus* and *P. acnes* are the most prevalent causative agents of SSTIs (1–4). In fact over 90% of the world's population will suffer from acne over the course of their lifetime, leading to annual direct costs of over $3 billion (1, 2, 5, 6). The threat of these pathogens is compounded by the tremendous rise in antibiotic resistance, reducing the efficacy of the existing antibacterial armamentarium (1, 3, 4). Identifying new drug targets to treat SSTIs is paramount to enable the development of novel therapeutics.

Heme biosynthesis is conserved across all domains of life, and heme is used for a diverse range of processes within cells. Until recently, it was thought that the heme biosynthesis pathway was conserved across all species, limiting its utility as a potential therapeutic target to treat infectious diseases. However, Dailey et al. (7, 8) discovered that Gram-positive bacteria use a distinct pathway to synthesize the critical cellular cofactor heme (Fig. 1*A*). Specifically, Gram-positive heme biosynthesis diverges at the conversion of coproporphyrinogen III (CPGIII) to coproporphyrin III (CPIII) through a six-electron oxidation by coproporphyrinogen oxidase (CgoX, formally known as HemY), as opposed to being converted to protoporphyrin IX (PPIX) in the classical pathway by a distinct series of enzymes (7, 9, 10). The divergence of the heme biosynthesis machinery between humans and Gram-positive bacteria provides a unique opportunity for the development of antibiotics targeting this pathway as a strategy to treat infections.

Small-molecule VU0038882 ('882) was previously identified in a screen for activators of the *S. aureus* heme-sensing system two-component system (HssRS) (11–13) (Fig. 1*B*). Upon activation, HssRS induces the expression of the heme-regulated transporter (HrtAB) to alleviate heme toxicity (11–13). HssRS activation is triggered by massive accumulation of heme in '882-exposed bacteria (11). In addition to activating HssRS, treatment with '882 induces toxicity to bacteria undergoing fermentation by impacting iron–sulfur cluster biogenesis (11, 14). Through a medicinal chemistry approach, the HssRS-activating properties of '882 were decoupled from its toxicity, suggesting two distinct cellular targets for this small molecule (11, 14, 15). Before this investigation, the mechanism by which '882 activates heme biosynthesis to trigger HssRS had not been uncovered.

We report here the identification of the cellular target of '882 responsible for inducing heme biosynthesis through the use of a P_{hrt}-driven suicide strain. '882 activates CgoX from Gram-positive bacteria, an enzyme essential for heme biosynthesis. Activation of CgoX induces accumulation of the product of the

Significance

Skin and soft tissue infections (SSTIs) account for a majority of visits to hospitals and clinics in the United States and are typically caused by Gram-positive pathogens. Recently, it was discovered that Gram-positive bacteria use a unique pathway to synthesize the critical cellular cofactor heme. The divergence of the heme biosynthesis pathways between humans and Gram-positive bacteria provides a unique opportunity for the development of new antibiotics targeting this pathway. We report here the identification of a small-molecule activator of coproporphyrinogen oxidase (CgoX) from Gram-positive bacteria that induces accumulation of coproporphyrin III and leads to photosensitization of Gram-positive pathogens. In combination with light, CgoX activation reduces bacterial burden in murine models of SSTI.

Author contributions: M.C.S., L.J.L., G.A.S., H.A.D., and E.P.S. designed research; M.C.S., D.J.H., L.J.L., A.R.F., J.S., and K.J.S. performed research; B.F.D., J.B.F., J.L.J., R.N., P.L.T., M.A., I.S.G., E.D.J., G.A.S., D.B.L., and H.A.D. contributed new reagents/analytic tools; M.C.S., D.J.H., L.J.L., A.R.F., K.J.S., J.B.F., J.L.J., E.D.J., D.B.L., and E.P.S. analyzed data; and M.C.S., D.J.H., and E.P.S. wrote the paper.

Conflict of interest statement: M.C.S., B.F.D., G.A.S., and E.P.S. have filed a patent for the small-molecule activity reported in this paper.

This article is a PNAS Direct Submission. F.C.F. is a guest editor invited by the Editorial Board.

Freely available online through the PNAS open access option.

[1]To whom correspondence should be addressed. Email: eric.skaar@vanderbilt.edu.

This article contains supporting information online at www.pnas.org/lookup/suppl/doi:10.1073/pnas.1700469114/-/DCSupplemental.

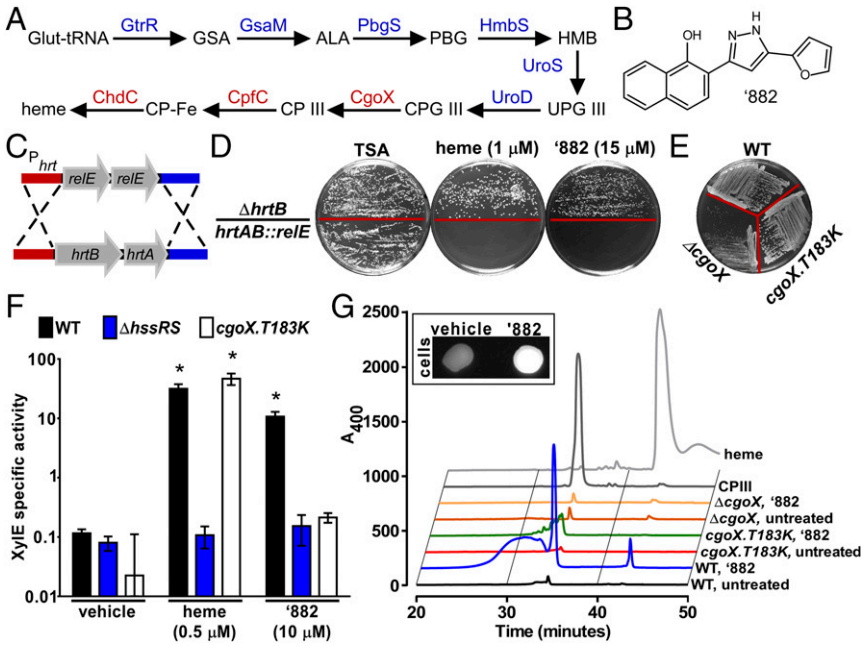

Fig. 1. '882 exposure increases CPIII production in *S. aureus*. (*A*) The terminal enzymes in the Gram-positive heme biosynthesis pathway (red) are distinct from other organisms. (*B*) '882 is a small molecule that increases heme biosynthesis in *S. aureus* (11). (*C*) To create a P_{hrt} suicide strain, the *hrtAB* genes were replaced with two copies of the *E. coli* gene encoding the RNA interferase toxin RelE. (*D*) Upon heme or '882 stimulation, toxicity is induced in *hrtAB::relE*. (*E*) Strain *CgoX.T183K* exhibits a normal growth phenotype on tryptic soy agar (TSA), suggesting the CgoX T183K does not restrict CgoX function. (*F*) Strain *CgoX.T183K* is unresponsive to '882, but retains the ability to respond to heme as measured by P_{hrt} activation. $^*P < 0.001$ compared with vehicle treated for each strain. (*G*) HPLC analysis of WT, *CgoX.T183K*, and Δ*CgoX* ± '882. '882 increases CPIII production in WT cells but not in *CgoX.T183K*. (*Inset*) '882-induced CPIII accumulation induces fluorescence in treated cells.

reaction, CPIII, a photoreactive molecule of demonstrated utility in treating bacterial infections (6, 16, 17). Photodynamic therapy (PDT) uses a photosensitizing molecule activated by a specific wavelength of light to produce reactive oxygen species that lead to cell death (6). Most US Food and Drug Administration-approved photosensitizers are aminolevulinic acid (ALA) derivatives, which serve as prodrugs through their conversion to porphyrins in the heme biosynthetic pathway (6). Through '882-dependent activation of CgoX, CPIII accumulates in a similar manner, inducing photosensitization specifically in Gram-positive bacteria, and '882-PDT reduces bacterial burden in murine models of SSTI (Fig. S1). Thus, small-molecule activation of CgoX represents a promising strategy for the development of light-based antimicrobial therapies.

Results

Construction of an '882-Responsive Suicide Strain. To identify the target of '882, a suicide strain was created enabling selection of *S. aureus* strains that are unresponsive to '882. Because '882 is not toxic to wild-type (WT) bacteria, a genetic approach was used to engineer toxicity to *S. aureus* upon treatment with '882. *S. aureus hrtAB* was replaced with two copies of the gene encoding the *Escherichia coli* RNA interferase toxin RelE under the control of the native *hrtAB* promoter to inhibit growth upon activation of HssRS (Fig. 1*C*). Dual copies of *relE* were used to avoid selection of toxin-inactivating mutations. *S. aureus hrtAB::relE* grows equivalently to WT in the absence of heme or '882. Upon HssRS induction by heme or '882, *hrtAB::relE* is unable to grow (Fig. 1*D*). A strain lacking the *hrtB* permease (Δ*hrtB*) was used to ensure that '882 does not induce heme toxicity at tested concentrations. These results establish this suicide strain as a powerful tool to identify suppressor mutants unresponsive to '882.

Selection of '882-Resistant Suicide Strains. Isolates of *hrtAB::relE* exhibiting spontaneous resistance to '882 were identified at a frequency of 0.0079%, and the stability of resistance was ensured through serial passage. Genomic DNA was isolated and the *hssRS*/*hrtAB* locus was sequenced. Whole-genome sequencing was performed on isolates lacking mutations in *hssRS*/P*hrt* to identify mutations conferring resistance to '882 in the *hrtAB::relE* strain background. This analysis revealed a T183K mutation in CgoX, an enzyme required for heme biosynthesis. The CgoX T183K mutation was reconstructed in WT *S. aureus* (*CgoX.T183K*), and this strain exhibits normal growth, suggesting the CgoX T183K mutation prevents the response of *S. aureus* to '882 without restricting heme biosynthesis, as seen in a strain lacking CgoX (Δ*CgoX*) (18) (Fig. 1*E*). In addition, the T183K mutation abolished '882 sensing to the same level as Δ*hssRS*, whereas heme sensing remained intact (Fig. 1*F*). Taken together, these results demonstrate that the CgoX T183K mutation prevents '882-induced activation of *hrtAB* in *S. aureus*.

'882 Induces CPIII Accumulation. To determine the impact of '882 on the heme biosynthesis pathway, intermediates of heme biosynthesis were quantified following '882 exposure. Porphobilinogen (PBG), an early heme biosynthetic precursor, is unaffected by '882 (Fig. 1*A* and Fig. S2). In contrast, CPIII, the product of CgoX, is greatly increased following '882 treatment (Fig. 1 *A* and *G*). Notably, CPIII accumulation is not observed in *CgoX.T183K* or Δ*CgoX* upon '882 treatment (Fig. 1*G*). CPIII is the only fluorescent molecule in the heme biosynthesis pathway, and '882 exposure triggers dramatic fluorescence in *S. aureus* (Fig. 1*G*, *Inset*). The HPLC fraction corresponding to the elution time of the CPIII standard was analyzed by LC-MS/MS and confirmed to be CPIII (Fig. S3). These results demonstrate that '882 exposure leads to accumulation of CPIII in *S. aureus* and implicate CgoX as a candidate target of the molecule.

'882 Activates CgoX from Gram-Positive Bacteria in Vitro. To determine whether '882 directly activates *S. aureus* CgoX, recombinant *S. aureus* WT CgoX and CgoX T183K were purified. Importantly,

these two enzymes display similar K_m and V_{max} values, demonstrating the T183K mutation does not affect baseline CgoX activity (Fig. 2*G* and Fig. S4*A*). Upon treatment with '882, WT CgoX displayed 205% activity with an AC_{150} of 92 nM, whereas the T183K mutant did not respond to '882 at concentrations up to 10 μM (Fig. 3 *A* and *G*). These data establish '882 as a small-molecule activator of CgoX.

To determine whether '882 retains activity against CgoX from other Gram-positive organisms, recombinant *Bacillus subtilis* and *P. acnes* CgoX were purified (7). K_m and V_{max} values were determined to characterize baseline activity of the enzymes, and each was tested for '882-induced activation (Fig. 2 *B* and *G* and Fig. S4*B*). '882 activates CgoX from *B. subtilis* and *P. acnes* with AC_{150} values of 42 and 16 nM, respectively (Fig. 2 *B* and *G*). Importantly, human HemY, a protoporphyrinogen oxidase as opposed to a coproporphyrinogen oxidase, did not respond to '882 treatment (Fig. 2*C* and Fig. S4*C*). These results establish '882 as a small-molecule activator of CgoX from Gram-positive bacteria.

Structure–Activity Relationship Studies of '882. Recently, a series of structural analogs of '882 were prepared and screened in a phenotypic HssRS activation assay using a XylE reporter gene to monitor transcription of *hrtAB* as a response to heme accumulation

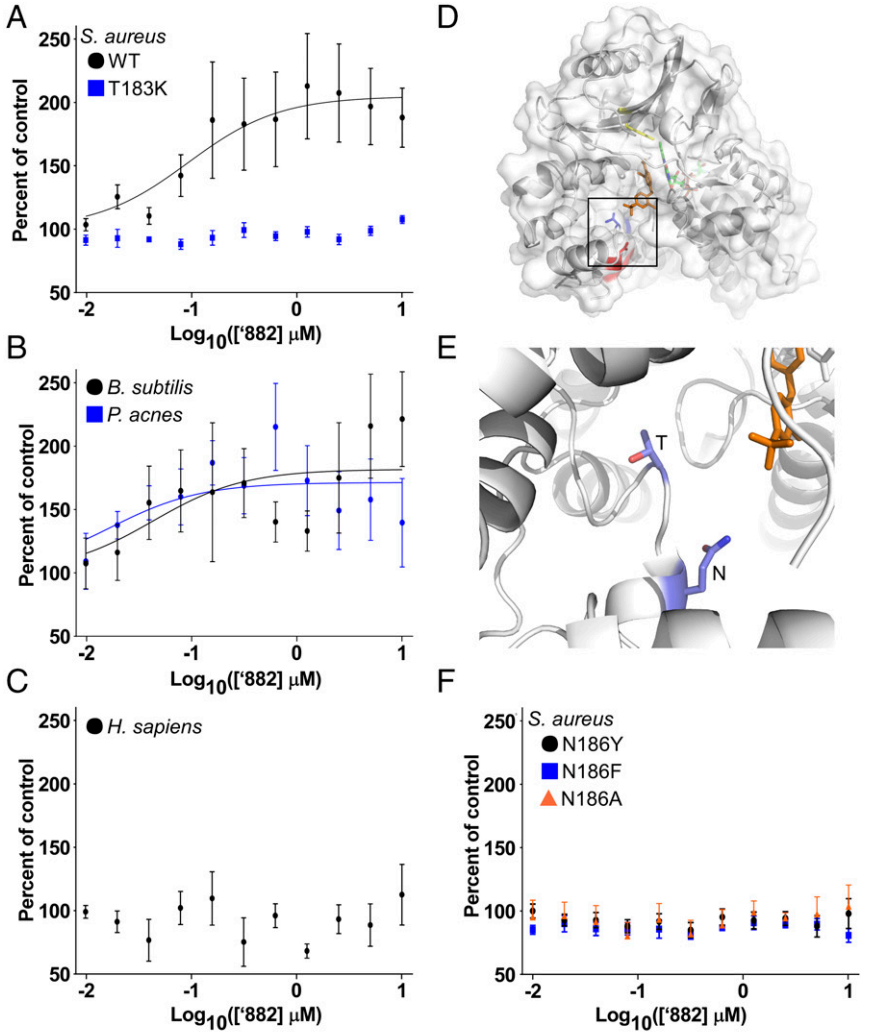

G

	K_M (μM, SE)	V_{max} (f.u./min, SE)	AC_{150} (nM, SE)	Activation (%)
***S. aureus* WT**	9.3 (6.6)	5.3 (1.7)	92.3 (29.3)	204.8 (6.8)
***S. aureus* T183K**	8.1 (4.3)	4.6 (1.1)	>10 μM	N/A
B. subtilis	20.8 (7.8)	28.5 (6.6)	42.7 (36.4)	181.7 (12.6)
P. acnes	23.4 (20.9)	18.4 (10.5)	16.7 (14.2)	171.2(9.2)
H. sapiens	2.3 (0.5)	2.1 (0.1)	>10 μM	N/A
***S. aureus* N186Y**	73.3 (61.1)	34.0 (23.7)	>10 μM	N/A
***S. aureus* N186F**	ambig	ambig	>10 μM	N/A
***S. aureus* N186A**	ambig	ambig	>10 μM	N/A

Fig. 2. '882 activates CgoX from Gram-positive bacteria and identification of a region important for regulation of CgoX. (*A*, *B*, and *F*) CgoX activity was assayed with increasing '882 concentrations and 5 μM CPGIII. (*C*) HemY activity was assayed with increasing '882 concentrations and 5 μM PPGIX. (*D*) The residue of *B. subtilis* CgoX homologous to *S. aureus* T183 (blue) is located in a region distinct from the active site (Y366, yellow) (19, 51). *B. subtilis* CgoX shares 46% identity with *S. aureus* CgoX. A residue homologous to *S. aureus* N186 (red) faces a cleft leading into the active site. (*E*) Magnified view of residues homologous to *S. aureus* T183 and N186 residues (carbon in light blue, nitrogen in dark blue, and oxygen in red). (*G*) K_m, V_{max}, AC_{150}, and activation (in percentage) for each enzyme were determined.

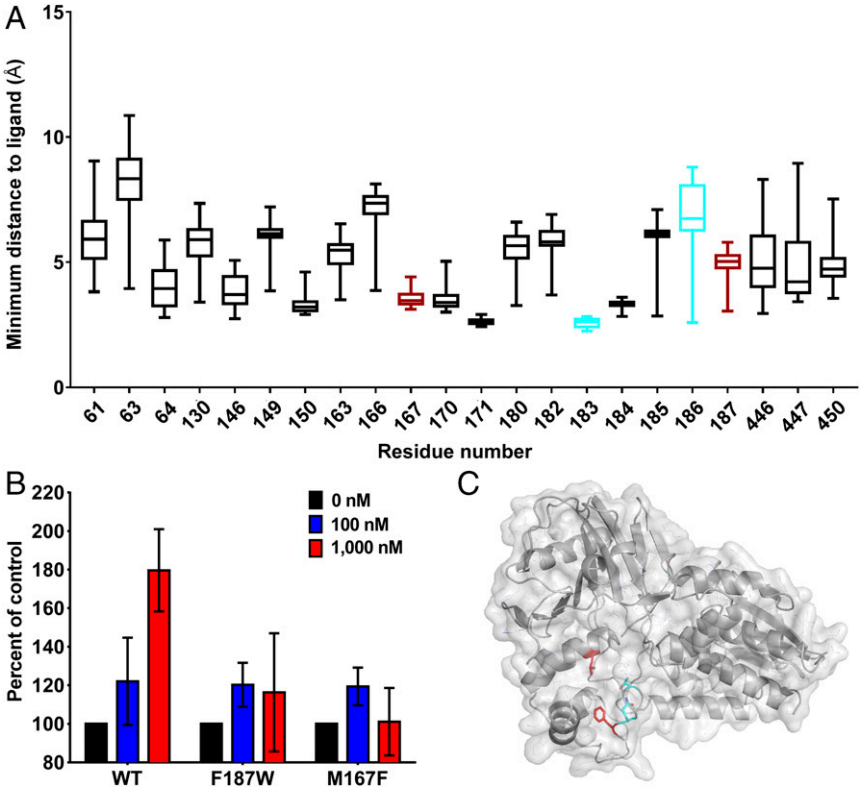

Fig. 3. Identification of additional mutations that affect '882 activity. (*A*) Distribution of ligand–residue distances for the subset of protein residue positions for which at least one of the top 100 ligand conformations was within 4 Å, shown as boxplots (box represents 25th and 75th percentile, and the horizontal line inside the box represents the median; vertical bars span between the min and max values). The two residues used to guide the docking are shown in cyan, whereas the two additional residues that were identified by the modeling approach and confirmed to have the desired disruption of '882 activity are shown in red. Structural analysis was performed on the *B. subtilis* crystal structure; homologous residue numbers to the *S. aureus* sequence are displayed (19). (*B*) CgoX activity was assayed with '882 and 5 μM CPGIII. (*C*) Structural model highlighting the same four residues as in the boxplot in the *B. subtilis* structure (19).

(15) (Table 1). These analogs were assayed in the CgoX activation assay using WT and T183K mutant enzymes (Table 1). Three analogs, b, d, and l, proved superior or comparable to '882 as CgoX activators in vitro. Notably, none of these more potent activators exhibit increased ability to trigger *hrtAB* expression in *S. aureus* over that of '882, suggesting that these compounds do not have improved bioavailability over '882 in staphylococcal cells. In addition, these '882 derivatives are also inactive against the T183K mutant, suggesting all four diarylpyrazoles share a common binding site. The remaining eight diarylpryazoles were equally inactive when assayed against CgoX or the T183K mutant. Collectively, these structure–activity relationship studies support activation of CgoX by a common allosteric binding site.

Structural Analysis of the '882–CgoX Interaction. To gain insight into the potential binding site of '882 within CgoX, the previously solved crystal structure of *B. subtilis* CgoX was interrogated (19) (Fig. 2*D*). Based on the location of *S. aureus* T183 within CgoX, a nearby amino acid, N186, was implicated as potentially important due to its proximity on a short helix facing a cleft leading into the active site (Fig. 2 *D* and *E*). The N186 residue was mutated to tyrosine, phenylalanine, or alanine and the activity of the mutant enzyme was examined in the presence or absence of '882 (Fig. 2 *F* and *G* and Fig. S4*D*). CgoX N186Y and CgoX N186F exhibit increased baseline activity relative to WT CgoX, suggesting this region is important for positive enzyme regulation (Fig. 2*G* and Fig. S4*D*). Consistent with this, all three mutations abolish the ability of CgoX to respond to '882 treatment (Fig. 2 *F* and *G*). Importantly, the helix containing these residues is in a distinct region from the active site of the molecule (Fig. 2*D*). Taken together, these data support a model whereby '882 binds to the region of CgoX containing residues 183–186 and acts as an allosteric modulator of enzyme activity. Mutations in this portion of the enzyme may mimic '882-induced changes in tertiary structure leading to enzyme activation.

In Silico Docking Identifies a Functional Domain Important for '882 Activation. Despite significant efforts, we were unsuccessful in our attempts to solve the complete crystal structure of '882 in complex with CgoX from various Gram-positive organisms. A flexible loop encompasses residues 183–186 that were identified in our initial mutational analysis. Importantly, previously published structures of CgoX are also incomplete in this region (19, 20). Therefore, to further our understanding of the functional domain required for '882 activity in the absence of a crystal structure, the '882–CgoX interaction was modeled by in silico docking to identify additional residues that may be required for '882-induced activity of CgoX. Based upon this analysis, six more residues within CgoX were selected for mutational analysis to interrogate their importance for '882-dependent activation (Fig. 3*A*). Mutations were made in *S. aureus* CgoX, creating the enzyme variants V146M, M167F, Y171A, F184A, F187W, and D450Y. Upon induction, V146M, Y171A, F184A, and D450Y led to unstable enzymes that could not be purified (Fig. S5). CgoX M167F and F187W expressed equivalently to WT (Fig. S5), were purified, and interrogated for '882-induced activation. Both mutations inhibited the activation of CgoX by '882 (Fig. 3*B*). Taken together, these data begin to define a pocket within

Table 1. Structural analogs of '882 activate HemY

Structure	Compound designation	Compound abbreviation	In vivo activity: % activity of '882 at 50 μM (SEM)	In vitro activity: % activity of WT HemY at 1 μM (SEM)	In vitro activity: % activity of T183K HemY at 1 μM (SEM)
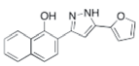	VU0038882	a	100 (9)*	192 (21)	69.3 (8.8)
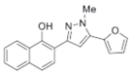	VU0812197	b	0.335 (0.276)*	300 (42)	72.3 (11.5)
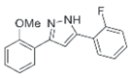	VU0420372	c	1.67 (0.55)*	230 (40)	72.1 (7.5)
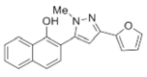	VU0812187	d	0.206 (0.113)*	153 (15)	35.7 (4.7)
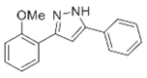	VU0420382	e	0.812 (0.297)*	128 (12)	78.3 (7.9)
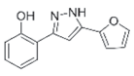	VU0125897	f	28.2 (0.8)*	112 (16)	110 (19)
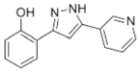	VU0476720	g	0.392 (0.146)*	111 (13)	95.6 (9.7)
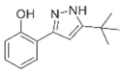	VU0476725	h	0.299 (0.188)*	109 (17)	137 (12)
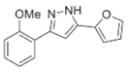	VU0366053	i	0.715 (0.093)*	89.6 (11.4)	106 (12)
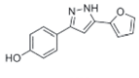	VU0404345	j	1.19 (0.31)*	81.9 (24.4)	75.8 (10.0)
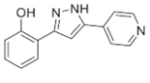	VU0476722	k	0.286 (0.136)*	79.4 (9.0)	95.2 (15.2)
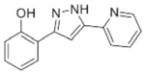	VU0812191	l	0.245 (0.036)*	77.8 (14.9)	72.1 (9.5)

*Previously published data (15).

CgoX that appears to be required for '882-dependent activation of the enzyme (Fig. 3*C*).

CgoX Activation Induces Photosensitization of Gram-Positive Bacteria. PDT is frequently used to treat bacterial skin infections and involves the use of a photosensitizer and a light source to destroy cells through the production of reactive oxygen species (6). Porphyrin intermediates of the heme biosynthesis pathway are the most common photosensitizers used in clinics. The production of porphyrin intermediates is often up-regulated through the addition of ALA, the first committed precursor in the heme biosynthetic pathway (Fig. 1*A*). A major limitation of ALA-PDT for the treatment of infectious diseases is the lack of specificity of this therapy, which induces photosensitivity in both bacterial and human cells. Due to the specificity of '882 for CgoX from Gram-positive bacteria, this molecule should selectively sensitize bacteria to light while avoiding host toxicity. To test this hypothesis, various strains of *S. aureus* were grown in the presence of ALA, '882, or both and exposed to 395-nm light, the absorbance maximum for CPIII as determined experimentally (data not shown). Both ALA and '882 treatment led to significant growth inhibition of *S. aureus* following exposure to 68 J/cm^2 light (Fig. 4*A*). An additive effect was seen when '882 and ALA were in combination, likely due to ALA increasing precursor availability for CgoX. Notably, ALA and '882 combined decreased *S. aureus* viability by six logs compared with untreated cells (Fig. 4*A*). The toxicity of '882-PDT is conserved across some of the most important causes of human skin infections, including *S. epidermidis*, *Staphylococcus haemolyticus*, *Staphylococcus lugdunensis*, *B. anthracis*, and *P. acnes* (Fig. 4 *B–D*). These results establish the utility of '882-PDT as a potential therapeutic for the treatment of skin infections caused by Gram-positive bacteria.

'882-PDT Decreases Bacterial Burdens in Vivo. To determine the in vivo efficacy of '882-PDT, a murine model of superficial *S. aureus* skin infection was used, which leads to considerable skin ulceration (21). Mice infected with *S. aureus* USA300 LAC and treated with '882-PDT or '882/ALA-PDT exhibited significantly lower bacterial burden per wound following infection compared with untreated animals (Fig. 4*G*). Histologically, all groups showed varying degrees of inflammation, with neutrophils being the most abundant cells present; however, bacterial burden was noticeably reduced in '882-PDT- and '882/ALA-PDT-treated samples (Fig. 4 *E* and *F*). Topical administration of 2% mupirocin ointment, as a positive control antibiotic, also significantly reduced bacterial burden compared with untreated mice. (Fig. 4*G*).

To evaluate the broad utility of '882-PDT as a therapy for common skin infections, the efficacy of '882-PDT in a murine

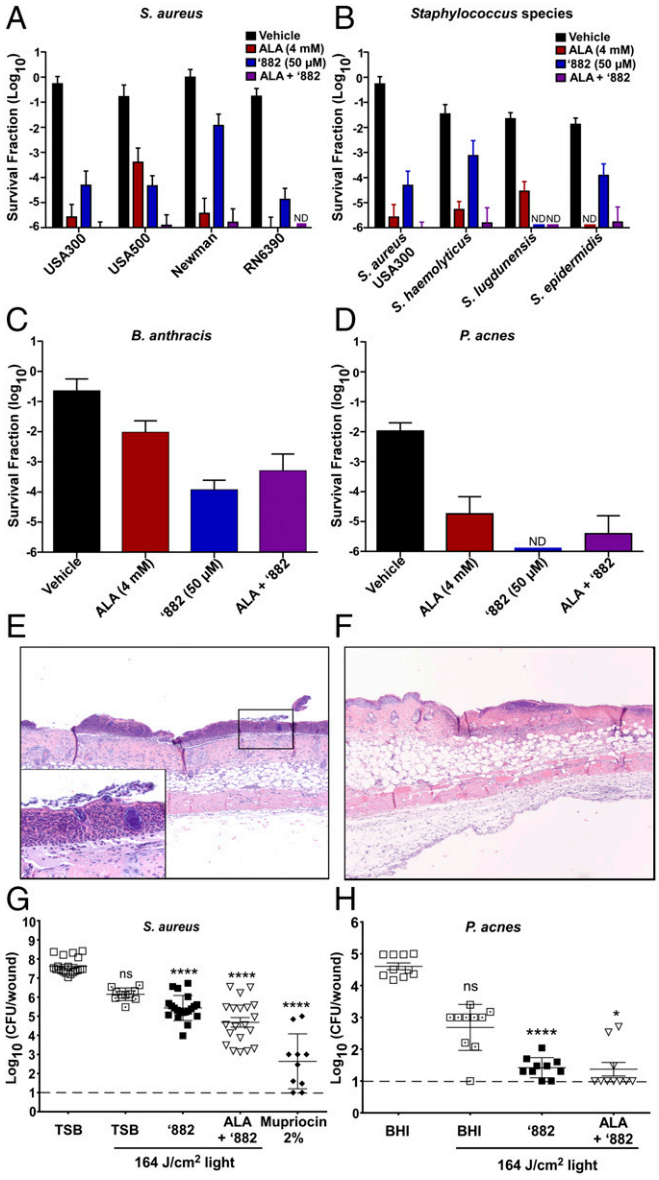

Fig. 4. '882 induces photosensitivity in Gram-positive pathogens. (*A–H*) *S. aureus*, *S. epidermidis*, *S. haemolyticus*, *S. lugdunensis*, *B. anthracis*, and *P. acnes* were exposed to ALA, '882, or ALA plus '882 in the absence or presence of 68 J/cm^2 light dose (395 nm). The survival fraction ± SD (*A–D*) was calculated by taking the number of surviving CFU of the light-exposed bacteria divided by the CFU of untreated bacteria (n = 9). (*E–G*) Mice infected with *S. aureus* USA300 LAC were treated with '882 (n = 20), ALA plus '882 (n = 20), 2% mupirocin ointment (n = 10), or left untreated in the absence (n = 20) or presence (n = 10) of a total dose of 164 J/cm^2. (*G*) Total $\log_{10}$ bacterial burden per wound ± SEM was quantified 16 h postinfection. (*E*) Section (10×; TSB 0 J/cm^2) shows a severe, neutrophilic epidermitis with a thick serocellular crust including coccal bacterial colonies [see *Inset* (40×)]. Inflammatory cells are primarily neutrophils and to a lesser extent mononuclear leukocytes and extend into the dermis and dermal adipose. (*F*) This section (10×; ALA plus '882 plus 164 J/cm^2) shows a margin of wounded epithelium and the adjacent nontreated epithelium. The treated portion has a layer of neutrophils just below the epidermis. Neutrophils and mononuclear leukocytes are present within the underlying dermal fibrous connective tissue, adipose tissue, and extending into the loose connective tissue below the muscle. (*H*) Mice infected with *P. acnes* were treated with either '882 or a combination of ALA and '882 in the absence or presence of a total dose of 164 J/cm^2 (each group = 10). Total $\log_{10}$ bacterial burden per wound ± SEM was enumerated 16 h postinfection. (*G* and *H*) Dashed lines indicate the limit of the detection for bacterial burden.

model of *P. acnes* infection was determined. Both '882-PDT and '882/ALA-PDT led to a significant decrease in bacterial burden compared with untreated mice, highlighting the utility of '882 as a possible compound for the treatment of acne (Fig. 4*H*). Taken together, these findings establish PDT coupled with small-molecule activation of CgoX as an effective therapeutic strategy to specifically target Gram-positive pathogens.

Discussion

These results define the small-molecule '882 as an activator of Gram-positive CgoX. Treatment with '882 leads to massive heme accumulation resulting in HssRS activation in *S. aureus*. Residues required for '882-induced CgoX activation have been identified, thereby revealing a functional domain involved in the activation of CgoX. In addition, treatment with '882 leads to photosensitization of Gram-positive bacteria, reducing bacterial burdens in vivo. Taken together, these results establish '882 as an activator of Gram-positive CgoX and provide proof-of-principle for small-molecule activation of CgoX as a potential therapeutic strategy for the treatment of bacterial infections.

Synthetic small-molecule activators are rare, with only a handful identified to date (22). Identifying the targets of small molecules is a major obstacle in biomedical research (23–25). Phenotypic high-throughput screens using small-molecule libraries often result in the identification of numerous molecules with unknown targets. Several approaches have been successful in identifying intracellular targets of small molecules (26–32). Here, we report a genetic selection strategy based on the creation of a suicide strain that enables the identification of spontaneous resistant mutants to an activating compound that is typically nontoxic. This strategy can be adapted to a variety of systems where a small molecule activates a specific gene expression program, and may enable the identification of targets for numerous small-molecule activators.

The mechanisms by which heme biosynthesis is regulated in Gram-positive bacteria are largely unknown (9). The identification of '882 as an activator of CgoX establishes this molecule as a valuable tool for interrogating the heme biosynthetic pathway in Gram-positive bacteria to further understand the synthesis of this essential cofactor. Interestingly, it has previously been demonstrated that CgoX activity is modulated in vitro to a similar extent by addition of ChdC (previously known as HemQ), the terminal enzyme in the Gram-positive heme biosynthesis pathway (33). This suggests that the interaction of CgoX with '882 may not be a random occurrence but may represent an inappropriate hijacking of a normal in vivo regulatory mechanism. The '882-dependent activation of heme biosynthesis represents a valuable tool for studying the regulation of heme biosynthesis in Gram-positive bacteria.

Notably, enzyme activators have numerous properties that make them ideal therapeutics (22). Whereas inhibitors often require the ability to inhibit the enzyme by 90%, activators can induce phenotypes with small increases in enzyme activity, indicating that derivatives of '882 with slight increases in activity could lead to dramatic increases in CPIII accumulation and therefore antibacterial properties (22). Specifically, this has been seen with small-molecule activators of glucokinase, where a 1.5-fold increase in enzymatic activity has shown significant effects in vivo. These molecules are now used as therapeutics for diabetes (22, 34–36).

In addition, inhibitors often bind active sites of enzymes, which are typically well conserved across homologous enzymes. In contrast, activators often bind allosteric sites, which are less well conserved across enzymes, thus increasing specificity and limiting off-target effects (22, 34, 37). Structural analysis of the '882–CgoX interaction has identified a functional domain of CgoX that suggests an allosteric mechanism of action for '882-induced activation (Figs. 2 and 3). In addition, we have identified specific

residues that when mutated increase activity, further supporting that this portion of the enzyme is important in positive regulation (Fig. 2). Therefore, '882 and its derivatives have value as both probes of heme biosynthesis as well as small-molecule photosensitizers for the treatment of bacterial infections.

The use of PDT has begun to expand beyond SSTIs. Gastrointestinal endoscopes have been developed that emit wavelengths that activate porphyrins in patients to detect cancer, and similar strategies have been interrogated for their ability to treat gastrointestinal infections (38, 39). Osteomyelitis and contamination of orthopedic devices are some of the most common invasive bacterial infections, and PDT strategies to combat these infections are being developed (40–46). Finally, PDT-based strategies are in development for a variety of other diseases, including parasitic, dental, and sinus infections (47, 48). One of the key limitations for PDT approaches involving photosensitizers that need to be activated with light at shorter wavelengths (below 500 nm) is the lack of deep-tissue penetration of light at those wavelengths. Therefore, the development of strategies to increase the penetration of light may considerably improve the therapeutic potential of porphyrin-based PDT. As the utility of PDT-based therapies expands, so too will the potential clinical utility of small-molecule activators of CgoX.

The ability of '882 to specifically photosensitize Gram-positive bacteria circumvents the nonspecific nature of ALA-PDT, which has limited the value of ALA-PDT for the treatment of infectious diseases (6, 49, 50). Furthermore, this provides proof-of-concept that activation of bacterial porphyrin production through specific activation of CgoX is a viable therapeutic strategy that could be adapted to Gram-negative bacteria and other infectious diseases (6, 16, 47). Therefore, the development of '882-PDT has the potential to significantly expand the value of light-based therapies for the treatment of the most common causes of skin infections.

Materials and Methods

Descriptions of growth conditions, strain construction, suicide strain selection experiments, genomic analysis, heme precursor quantification, promoter activity assays, CgoX activity assays, in silico docking studies, photosensitivity assays, superficial skin infection studies, and chemical synthesis can be found in *SI Materials and Methods*. Bacterial strains, expression constructs, plasmids, and primers used in this study can be found in Tables S1–S4. All research involving animals described in this paper was reviewed and approved by the Vanderbilt University Institutional Animal Care and Use Committee.

ACKNOWLEDGMENTS. We thank members of the E.P.S. laboratory for critical reading of the manuscript. Core services performed through Vanderbilt University Medical Center's Digestive Disease Research Center were supported by NIH Grant P30DK058404 Core Scholarship. The following reagents were provided by the Network on Antimicrobial Resistance in *Staphylococcus aureus* for distribution by BEI Resources, National Institute of Allergy and Infectious Diseases, NIH: *Staphylococcus epidermidis* strain HIP04645 (NR-45860) and Nebraska Transposon Mutant Library Screening Array (NR-48501). This work was supported by Public Health Service Award T32 GM07347 from the National Institute of General Medical Studies for the Vanderbilt Medical-Scientist Training Program (to M.C.S. and P.L.T.), Grant R01 AI069233 (to M.C.S., L.J.L., and E.P.S.), Grant R01 AI073843 (to M.C.S. and E.P.S.), Grant T32 GM008554-18 (to L.J.L.), Grant T32 GM065086 (to B.F.D.), Grant R01 LM010685 (to P.L.T.), Grant T32 ES007028 (to M.A.), Vanderbilt Vaccine Center startup funds (to R.N. and I.S.G.), Vanderbilt University Medical Center Faculty Research Scholars award (to R.N. and I.S.G.), and Walter Reed Army Institute of Research Grant W81XWH-17-2-0003.

1. Tognetti L, et al. (2012) Bacterial skin and soft tissue infections: Review of the epidemiology, microbiology, aetiopathogenesis and treatment: A collaboration between dermatologists and infectivologists. *J Eur Acad Dermatol Venereol* 26:931–941.
2. Bhate K, Williams HC (2013) Epidemiology of acne vulgaris. *Br J Dermatol* 168: 474–485.
3. Dryden MS (2009) Skin and soft tissue infection: Microbiology and epidemiology. *Int J Antimicrob Agents* 34(Suppl 1):S2–S7.
4. Otto M (2013) Community-associated MRSA: What makes them special? *Int J Med Microbiol* 303:324–330.
5. Basra MK, Shahrukh M (2009) Burden of skin diseases. *Expert Rev Pharmacoecon Outcomes Res* 9:271–283.
6. Wan MT, Lin JY (2014) Current evidence and applications of photodynamic therapy in dermatology. *Clin Cosmet Investig Dermatol* 7:145–163.
7. Dailey HA, Gerdes S, Dailey TA, Burch JS, Phillips JD (2015) Noncanonical coproporphyrin-dependent bacterial heme biosynthesis pathway that does not use protoporphyrin. *Proc Natl Acad Sci USA* 112:2210–2215.
8. Lobo SA, et al. (2015) *Staphylococcus aureus* haem biosynthesis: Characterisation of the enzymes involved in final steps of the pathway. *Mol Microbiol* 97:472–487.
9. Choby JE, Skaar EP (2016) Heme synthesis and acquisition in bacterial pathogens. *J Mol Biol* 428:3408–3428.
10. Dailey HA, et al. (2017) Prokaryotic heme biosynthesis: Multiple pathways to a common essential product. *Microbiol Mol Biol Rev* 81:e00048-16.
11. Mike LA, et al. (2013) Activation of heme biosynthesis by a small molecule that is toxic to fermenting *Staphylococcus aureus*. *Proc Natl Acad Sci USA* 110:8206–8211.
12. Torres VJ, et al. (2007) A *Staphylococcus aureus* regulatory system that responds to host heme and modulates virulence. *Cell Host Microbe* 1:109–119.
13. Stauff DL, Torres VJ, Skaar EP (2007) Signaling and DNA-binding activities of the *Staphylococcus aureus* HssR-HssS two-component system required for heme sensing. *J Biol Chem* 282:26111–26121.
14. Choby JE, et al. (2016) A small-molecule inhibitor of iron-sulfur cluster assembly uncovers a link between virulence regulation and metabolism in *Staphylococcus aureus*. *Cell Chem Biol* 23:1351–1361.
15. Dutter BF, et al. (2016) Decoupling activation of heme biosynthesis from anaerobic toxicity in a molecule active in *Staphylococcus aureus*. *ACS Chem Biol* 11:1354–1361.
16. Maisch T, et al. (2011) Photodynamic inactivation of multi-resistant bacteria (PIB)–a new approach to treat superficial infections in the 21st century. *J Dtsch Dermatol Ges* 9:360–366.
17. Morimoto K, et al. (2014) Photodynamic therapy using systemic administration of 5-aminolevulinic acid and a 410-nm wavelength light-emitting diode for methicillin-resistant *Staphylococcus aureus*-infected ulcers in mice. *PLoS One* 9:e105173.
18. Proctor RA, et al. (2006) Small colony variants: A pathogenic form of bacteria that facilitates persistent and recurrent infections. *Nat Rev Microbiol* 4:295–305.
19. Qin X, et al. (2010) Structural insight into unique properties of protoporphyrinogen oxidase from *Bacillus subtilis*. *J Struct Biol* 170:76–82.
20. Corradi HR, et al. (2006) Crystal structure of protoporphyrinogen oxidase from *Myxococcus xanthus* and its complex with the inhibitor acifluorfen. *J Biol Chem* 281: 38625–38633.
21. Kugelberg E, et al. (2005) Establishment of a superficial skin infection model in mice by using *Staphylococcus aureus* and *Streptococcus pyogenes*. *Antimicrob Agents Chemother* 49:3435–3441.
22. Zorn JA, Wells JA (2010) Turning enzymes ON with small molecules. *Nat Chem Biol* 6: 179–188.
23. Lomenick B, et al. (2009) Target identification using drug affinity responsive target stability (DARTS). *Proc Natl Acad Sci USA* 106:21984–21989.
24. Ziegler S, Pries V, Hedberg C, Waldmann H (2013) Target identification for small bioactive molecules: Finding the needle in the haystack. *Angew Chem Int Ed Engl* 52: 2744–2792.
25. Burdine L, Kodadek T (2004) Target identification in chemical genetics: The (often) missing link. *Chem Biol* 11:593–597.
26. Palmer KL, Daniel A, Hardy C, Silverman J, Gilmore MS (2011) Genetic basis for daptomycin resistance in enterococci. *Antimicrob Agents Chemother* 55:3345–3356.
27. Kaatz GW, Lundstrom TS, Seo SM (2006) Mechanisms of daptomycin resistance in *Staphylococcus aureus*. *Int J Antimicrob Agents* 28:280–287.
28. Peleg AY, et al. (2012) Whole genome characterization of the mechanisms of daptomycin resistance in clinical and laboratory derived isolates of *Staphylococcus aureus*. *PLoS One* 7:e28316.
29. Meredith TC, Wang H, Beaulieu P, Gründling A, Roemer T (2012) Harnessing the power of transposon mutagenesis for antibacterial target identification and evaluation. *Mob Genet Elements* 2:171–178.
30. Wang H, Claveau D, Vaillancourt JP, Roemer T, Meredith TC (2011) High-frequency transposition for determining antibacterial mode of action. *Nat Chem Biol* 7:720–729.
31. Borden JR, Papoutsakis ET (2007) Dynamics of genomic-library enrichment and identification of solvent tolerance genes for *Clostridium acetobutylicum*. *Appl Environ Microbiol* 73:3061–3068.
32. Luesch H, et al. (2005) A genome-wide overexpression screen in yeast for small-molecule target identification. *Chem Biol* 12:55–63.
33. Dailey TA, et al. (2010) Discovery and characterization of HemQ: An essential heme biosynthetic pathway component. *J Biol Chem* 285:25978–25986.
34. Grimsby J, et al. (2003) Allosteric activators of glucokinase: Potential role in diabetes therapy. *Science* 301:370–373.
35. Bonadonna RC, et al. (2010) Piragliatin (RO4389620), a novel glucokinase activator, lowers plasma glucose both in the postabsorptive state and after a glucose challenge in patients with type 2 diabetes mellitus: A mechanistic study. *J Clin Endocrinol Metab* 95:5028–5036.
36. Bishop AC, Chen VL (2009) Brought to life: Targeted activation of enzyme function with small molecules. *J Chem Biol* 2:1–9.
37. Howitz KT, et al. (2003) Small molecule activators of sirtuins extend *Saccharomyces cerevisiae* lifespan. *Nature* 425:191–196.
38. Choi S, Lee H, Chae H (2012) Comparison of in vitro photodynamic antimicrobial activity of protoporphyrin IX between endoscopic white light and newly developed

narrowband endoscopic light against *Helicobacter pylori* 26695. *J Photochem Photobiol B* 117:55–60.
39. Hatogai K, et al. (2016) Salvage photodynamic therapy for local failure after chemoradiotherapy for esophageal squamous cell carcinoma. *Gastrointest Endosc* 83: 1130–1139.
40. Cassat JE, Skaar EP (2013) Recent advances in experimental models of osteomyelitis. *Expert Rev Anti Infect Ther* 11:1263–1265.
41. Gerber JS, Coffin SE, Smathers SA, Zaoutis TE (2009) Trends in the incidence of methicillin-resistant *Staphylococcus aureus* infection in children's hospitals in the United States. *Clin Infect Dis* 49:65–71.
42. Campoccia D, Montanaro L, Arciola CR (2006) The significance of infection related to orthopedic devices and issues of antibiotic resistance. *Biomaterials* 27:2331–2339.
43. Bisland SK, Burch S (2006) Photodynamic therapy of diseased bone. *Photodiagnosis Photodyn Ther* 3:147–155.
44. Bisland SK, Chien C, Wilson BC, Burch S (2006) Pre-clinical in vitro and in vivo studies to examine the potential use of photodynamic therapy in the treatment of osteomyelitis. *Photochem Photobiol Sci* 5:31–38.
45. Goto B, et al. (2011) Therapeutic effect of photodynamic therapy using Napheophorbide a on osteomyelitis models in rats. *Photomed Laser Surg* 29:183–189.
46. Li X, et al. (2013) Effects of 5-aminolevulinic acid-mediated photodynamic therapy on antibiotic-resistant staphylococcal biofilm: An in vitro study. *J Surg Res* 184: 1013–1021.
47. Dai T, Huang YY, Hamblin MR (2009) Photodynamic therapy for localized infections–State of the art. *Photodiagnosis Photodyn Ther* 6:170–188.
48. Krespi YP, Kizhner V (2011) Phototherapy for chronic rhinosinusitis. *Lasers Surg Med* 43:187–191.
49. Gholam P, Kroehl V, Enk AH (2013) Dermatology life quality index and side effects after topical photodynamic therapy of actinic keratosis. *Dermatology* 226:253–259.
50. Clark C, et al. (2003) Topical 5-aminolaevulinic acid photodynamic therapy for cutaneous lesions: Outcome and comparison of light sources. *Photodermatol Photoimmunol Photomed* 19:134–141.
51. Sun L, et al. (2009) Site-directed mutagenesis and computational study of the Y366 active site in *Bacillus subtilis* protoporphyrinogen oxidase. *Amino Acids* 37: 523–530.
52. Bae T, Schneewind O (2006) Allelic replacement in *Staphylococcus aureus* with inducible counter-selection. *Plasmid* 55:58–63.
53. Horton RM, Cai Z, Ho SM, Pease LR (1990) Gene splicing by overlap extension: Tailor-made genes using the polymerase chain reaction. *Biotechniques* 8:528–535.
54. Fey PD, et al. (2013) A genetic resource for rapid and comprehensive phenotype screening of nonessential *Staphylococcus aureus* genes. *MBio* 4:e00537–e12.
55. Mazmanian SK, et al. (2003) Passage of heme-iron across the envelope of *Staphylococcus aureus*. *Science* 299:906–909.
56. Fujita H (2001) Measurement of delta-aminolevulinate dehydratase activity. *Curr Protoc Toxicol* Chap 8:Unit 8.6.
57. Reniere ML, et al. (2010) The IsdG-family of haem oxygenases degrades haem to a novel chromophore. *Mol Microbiol* 75:1529–1538.
58. Weiner MP, et al. (1994) Site-directed mutagenesis of double-stranded DNA by the polymerase chain reaction. *Gene* 151:119–123.
59. Shepherd M, Dailey HA (2005) A continuous fluorimetric assay for protoporphyrinogen oxidase by monitoring porphyrin accumulation. *Anal Biochem* 344:115–121.
60. Morris GM, et al. (2009) AutoDock4 and AutoDockTools4: Automated docking with selective receptor flexibility. *J Comput Chem* 30:2785–2791.
61. Morris GM, et al. (1998) Automated docking using a Lamarckian genetic algorithm and an empirical binding free energy function. *J Comput Chem* 19:1639–1662.
62. Gao H, et al. (2015) Discovery of novel VEGFR-2 inhibitors. Part II: Biphenyl urea incorporated with salicylaldoxime. *Eur J Med Chem* 90:232–240.
63. Bender T, Huss M, Wieczorek H, Grond S, von Zezschwitz P (2007) Convenient synthesis of a [1-^{14}C]Diazirinylbenzoic acid as a photoaffinity label for binding studies of V-ATPase inhibitors. *Eur J Org Chem* 2007:3870–3878.
64. Duthie ES, Lorenz LL (1952) *Staphylococcal* coagulase; mode of action and antigenicity. *J Gen Microbiol* 6:95–107.
65. Attia AS, Benson MA, Stauff DL, Torres VJ, Skaar EP (2010) Membrane damage elicits an immunomodulatory program in *Staphylococcus aureus*. *PLoS Pathog* 6: e1000802.
66. Kreiswirth BN, et al. (1983) The toxic shock syndrome exotoxin structural gene is not detectably transmitted by a prophage. *Nature* 305:709–712.
67. Stauff DL, Skaar EP (2009) *Bacillus anthracis* HssRS signalling to HrtAB regulates haem resistance during infection. *Mol Microbiol* 72:763–778.
68. Sterne M (1946) Avirulent anthrax vaccine. *Onderstepoort J Vet Sci Anim Ind* 21: 41–43.
69. Dailey TA, Dailey HA (1996) Human protoporphyrinogen oxidase: Expression, purification, and characterization of the cloned enzyme. *Protein Sci* 5:98–105.